PHYSICAL REVIEW C **76**, 061601(R) (2007)

Distinctive features of Coulomb-related emissions in peripheral heavy ion collisions at Fermi energies

S. Piantelli,[1] P. R. Maurenzig,[2] A. Olmi,[1,*] L. Bardelli,[2] M. Bini,[2] G. Casini,[1] A. Mangiarotti,[2,†] G. Pasquali,[2] G. Poggi,[2] and A. A. Stefanini[2]

[1]*Sezione INFN di Firenze, Via G. Sansone 1, I-50019 Sesto Fiorentino, Italy*

[2]*Sezione INFN and Università di Firenze, Via G. Sansone 1, I-50019 Sesto Fiorentino, Italy*

(Received 27 June 2007; published 11 December 2007)

Light charged particles emitted at about 90° in the frame of the projectile-like fragment in semiperipheral collisions of ^{93}Nb+^{93}Nb at 38A MeV give evidence for the occurrence, in the same class of events, of two different production mechanisms. This is demonstrated by differences in the kinetic energy spectra and in the isotopic composition of the particles. The emission with a softer kinetic energy spectrum and a low N/Z ratio for the hydrogen isotopes is attributed to an evaporation process. The harder emission, with a much higher N/Z ratio, can be attributed to a midvelocity process consisting of a nonisotropic emission, on a short time-scale, from the projectile-like fragment.

DOI: 10.1103/PhysRevC.76.061601 PACS number(s): 25.70.Lm, 25.70.Pq

In peripheral and semiperipheral heavy ion collisions at Fermi energies a sizable fraction of the emitted light charged particles (LCPs) and intermediate mass fragments (IMFs, $Z \geqslant 3$) are produced at "midvelocity", i.e., they have velocities intermediate between those of the projectile-like fragment (PLF) and of the target-like fragment (TLF) (see, e.g., [1–7]). The midvelocity emissions represent a new, distinctive feature of the Fermi energy domain; for a review and an extensive list of references see [8]. However, in spite of many efforts, a comprehensive description of its characteristics and evolution with bombarding energy is still lacking, and also the nature of its production mechanism, whether statistical or dynamical, is still a debated matter.

One of the main difficulties, especially on the low energy side of the Fermi energy region, is separating the midvelocity emissions from the evaporation of PLF and TLF. For this purpose, one usually assumes a nearly isotropic distribution of the evaporated LCPs in the rest frame of the emitting PLF (and TLF) (indeed, for moderate spins, the out-of-plane anisotropy is rather weak). Then, the procedure (see, e.g., [2,5]) consists in attributing the forward emissions in the PLF frame to an isotropic evaporation from the PLF, extrapolating it to all angles and finally subtracting it from the total measured distribution: whatever yield remains in excess of the evaporation is ascribed to midvelocity mechanisms. The resulting emission pattern for midvelocity products is usually displayed in the $(v_\parallel, v_\perp)$ plane, where $v_\parallel$ ($v_\perp$) is the parallel (perpendicular) component of their c.m. velocity with respect to the PLF-TLF separation axis (or, sometimes, the beam axis). Close examination of this emission pattern suggests that in peripheral and semiperipheral collisions the midvelocity emissions consist not only of a broad distribution roughly centered at velocities intermediate between PLF and TLF, but also of an anisotropic emission [1,5,9,10], located along the Coulomb ridge of the PLF (and of the TLF as well). With increasing bombarding energy, the velocity gap between PLF and TLF opens up and the central component tends to fade away, while that along the Coulomb ridge stands up more clearly [11].

One can imagine different mechanisms which might contribute. Early emissions—such as, e.g., preequilibrium particles from the very first phases of the collision, or particles from the hot zone of overlapping matter during contact—are expected to populate mainly the central midvelocity region, possibly with large transverse momenta. Later emissions in the separation phase (or immediately after separation) are likely to display an increasingly strong relationship with just one of the reaction partners, so they are expected to show a kind of partial "orbiting" and to be mainly distributed, in a nonisotropic way, on the Coulomb ridge of one reaction partner (usually experiments concentrate on the PLF), preferentially facing the other one (the TLF). These later emitted Coulomb-related particles may just be neck remnants, left behind by a dynamical multiple neck-rupture process [12]; or they may be produced, after neck rupture, by the fast nonequilibrated decay of a possibly strongly deformed PLF, in a process resembling a fast oriented fission [13–15] for extreme mass asymmetries [3,7]. In this sense they have been attributed to a "surface" emission from the main reaction partners [3]. Different interpretations ascribe these later emissions to a pure statistical evaporation from the PLF, however perturbed by the proximity of the TLF [9,16].

In this Rapid Communication we put into evidence some distinctive features of this midvelocity component, which has been measured in a common angular range together with the PLF evaporation, in particular for what concerns the kinetic energy spectra of LCPs and the average isotopic composition of the $Z = 1$ particles. They may help constraining models on midvelocity processes.

The experimental data refer to the symmetric collision ^{93}Nb+^{93}Nb at 38A MeV, studied with the FIASCO setup (for details see [3,5,17]) at the Superconducting Cyclotron of the

*olmi@fi.infn.it

†Present address: Laboratório de Instrumentação e Física Experimental de Partículas, 3004-516 Coimbra, Portugal.

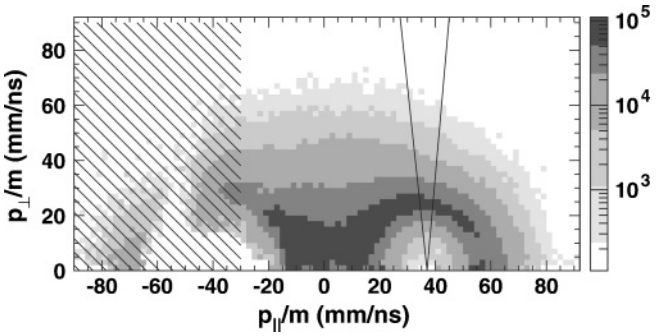

FIG. 1. Invariant cross section of α-particles in the plane ($\frac{p_\parallel}{m}$, $\frac{p_\perp}{m}$) of the c.m. frame, at TKEL = 550–650 MeV; the angular sector for the evaluation of the energy spectra is also shown (see text). The hatched area indicates the region with limited coverage of the setup.

Laboratori Nazionali del Sud of INFN in Catania. Attention is focused on two-body semiperipheral reactions, where the PLF and TLF emission patterns can be clearly separated. These reactions are selected by requiring only two heavy ($Z \gtrsim 10$) fragments in the exit channel, namely, the PLF and TLF (the latter one is efficiently detected even in the most peripheral collisions due to the low thresholds of the gas detectors).

For sorting purposes, we use the "Total Kinetic Energy Loss", a parameter obtained from the kinematic coincidence analysis [18] and defined as $\mathrm{TKEL} = E_{\mathrm{in}}^{\mathrm{c.m.}} - \frac{1}{2}\tilde{\mu}v_{\mathrm{rel}}^2$, where $E_{\mathrm{in}}^{\mathrm{c.m.}}$ is the center-of-mass energy in the entrance channel, v_{rel} the PLF-TLF relative velocity and $\tilde{\mu}$ the reduced mass assuming an exactly binary reaction. As noted in [5], at Fermi energies TKEL does not represent any more a good estimate of the true total kinetic energy loss of the collision, but it is used just as an *ordering parameter* for sorting the events in bins of increasing centrality. More details on the use of TKEL as an impact parameter estimator can be found in Appendix A of [5].

As the solid angle coverage of FIASCO, although large, is significantly smaller than 4π, the yields of LCPs and IMFs are first corrected [5] for the limited geometrical coverage and for the low-energy identification thresholds. Then, using relativistic kinematics,[1] we obtain the emission patterns in the c.m. frame (the polar axis is the asymptotic PLF-TLF separation axis pointing in the direction of motion of the PLF). One can now examine the distribution of the parallel and perpendicular components of the reduced particle momenta with respect to the polar axis ($\frac{p_\parallel}{m}$ and $\frac{p_\perp}{m}$, respectively). As a typical example, Fig. 1 presents the invariant cross section of α particles in one bin of TKEL. One clearly sees the Coulomb hole and the Coulomb ridge around the PLF source (at $\frac{p_\parallel}{m} \approx$ 37 mm/ns); the corresponding features of the TLF are obscured by the inefficiencies of the setup. The most forward part of the pattern, with circular contour levels centered on the PLF, is due to the usual evaporation, while the large intensification in the region between PLF and TLF is due to the midvelocity

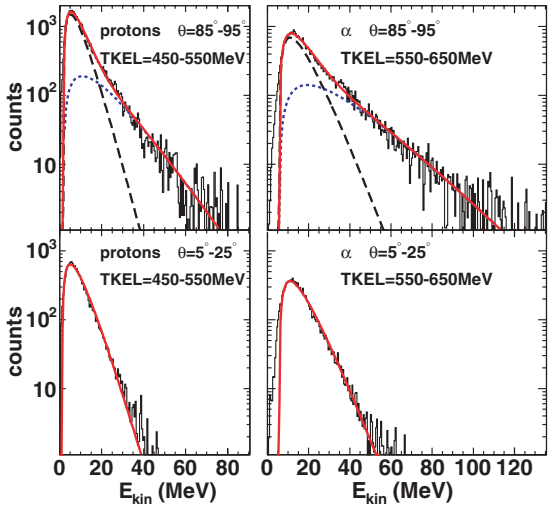

FIG. 2. (Color online) Kinetic energy spectra, in the reference frame of the PLF, for protons (left panels) at TKEL = 450–550 MeV and α particles (right panels) at 550–650 MeV. Upper and lower panels refer to particles emitted in the angular range $85^\circ \leqslant \theta \leqslant 95^\circ$ and $5^\circ \leqslant \theta \leqslant 25^\circ$, respectively. The full (red) curves are fits to the data with one effusive Maxwell function (lower panels) and with the superposition of two effusive Maxwell functions (upper panels), indicated by the dashed (black) and dotted (blue) curves.

emissions. Similar results are obtained for all particle species. A tail of midvelocity emissions extends even in the forward hemisphere of the PLF and produces both an anisotropy in the population of the Coulomb ridge and a marked deviation of the outer contour levels from the circular shape around the PLF.

A transformation into the PLF reference frame allows a better characterization of this tail. Moreover, for quantitative results one must choose a region where this midvelocity component has sufficient statistics, and this of course excludes too forward angles. At the same time it should not be obscured by the central midvelocity emissions and this excludes backward angles too. Thus, a not too wide angular region around 90° in the PLF reference frame (as indicated by the sector in Fig. 1) seems a good compromise. Here indeed the kinetic energy distributions of the particles show clear distinctive features. As an example, the upper panels of Fig. 2 show the kinetic energy spectra of protons at TKEL = 450–550 MeV (left) and α particles at 550–650 MeV (right). For comparison, the lower panels show the corresponding spectra for forward emitted particles. All spectra have been corrected for the angle-dependent effects caused by the recoil of the emitter (see [5] for more details). Such recoil effects are always relatively small and vanish around $\theta = 90^\circ$.

The distributions of forward emitted particles of the lower panels in Fig. 2 have been fitted with a single effusive Maxwell function, shown by the full (red) curve,

$$f_0(E) = N_0\left[(E - ZB_0)/T_0^2\right]\exp[-(E - ZB_0)/T_0], \quad (1)$$

with Z charge of the emitted particle, B_0 Coulomb barrier divided by Z and T_0 (inverse) slope parameter of the distribution. On the contrary, the distributions in the upper panels cannot be fitted with a single Maxwell function, but they can be fitted

[1] A relativistic transformation, instead of a Galileian one, is preferred to avoid distortions of the angular distribution of the fastest particles, in particular for protons, which may reach lab-velocities as large as $\beta = 0.3$.

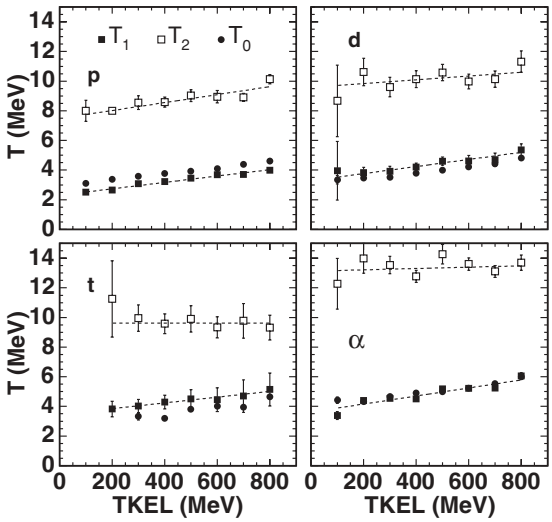

FIG. 3. Values of the slope parameters T_0 (filled circles), T_1 (filled squares), and T_2 (open squares) as a function of TKEL for protons, deuterons, tritons and α particles. The bars indicate just the statistical errors. Dashed lines through the filled and open squares are just to guide the eye.

with a two-component function

$$f_{12}(E) = N_1\left[(E - ZB_1)/T_1^2\right]\exp[-(E - ZB_1)/T_1] + N_2\left[(E - ZB_2)/T_2^2\right]\exp[-(E - ZB_2)/T_2] \quad (2)$$

with two different slope parameters T_1 and T_2 ($T_1 < T_2$) and equal barriers.[2] These two components are shown in Fig. 2 by the dashed (black) and dotted (blue) curves, respectively; the full (red) curve is their sum. No attempts were made to reproduce the smearing of the barriers, so the low-energy part of the histograms (below $\approx$70% of the peak height) is not used in the fit. Fits of similar quality are obtained for all LCPs at all TKEL values.

By simple inspection one sees that the slopes of the two components are quite different. For a quantitative comparison Fig. 3 presents T_1, T_2 and T_0 for all LCPs as a function of TKEL. The error bars are only statistical; further uncertainties (due, e.g., to efficiency and recoil corrections and to the choice of the fit region) are around 0.1–0.2 MeV for T_0 and 0.5–1.0 MeV for T_1 and T_2.

The values of the slope parameters of the harder component, T_2, are indeed definitely larger than T_1 and T_0. They are similar for all $Z = 1$ isotopes (around 8–11 MeV), while a still higher value (about 13 MeV) is found for α particles and also for IMFs (not shown in the figure; in this latter case, a fit with a single T_2 component is more appropriate, as the evaporation of IMFs from the PLF is negligible).

The second item worth noting is the quite similar values of T_0 and T_1. This leads to the conclusion that the softer component in the spectra at $\approx$90° (slope T_1, dashed curves in the upper panels of Fig. 2) can be attributed to the usual evaporation from the excited PLF. Actually, in the tail of the spectra at forward angles (lower panels of Fig. 2) there is a small excess of energetic particles (for protons and α particles, but not for deuterons and tritons), which might be due to a small pre-equilibrium contribution. A two-component fit with Eq. (2) would give a slope parameter of the evaporative component slightly smaller than the T_0 obtained with Eq. (1) and hence in even better agreement with T_1, at the expense of an increased uncertainty in the parameters of the second component.

The slope parameters of the evaporative process, T_0 and T_1, display a weak, almost linear, increasing trend with increasing TKEL. For all particles, the values are rather similar and vary in the range from 2.5 to 6 MeV. These values and their dependence on the violence of the collision are in good agreement with those of other studies focused just on the decay of projectile residues in peripheral collisions at Fermi energies [19,20]. In the first bins of TKEL, the values of T_1 are somewhat larger than those expected on the base of a simple Fermi-gas formula, using the estimate of $E^\star$ from [5]. However, T_0 and T_1 are just slope parameters. A connection with nuclear "temperatures" is particularly difficult in peripheral collisions at Fermi energies, due to the finite width of the distributions both in initial mass and excitation energy of the emitters and to uncertainties in the determination of the origin of the PLF frame. These effects are discussed in detail in Ref. [21], with regard to the decay of PLFs produced in peripheral collisions at Fermi energies and detected with the INDRA multidetector.

The harder component with slope T_2 cannot be a tail of the TLF evaporation (this source is too far away in velocity space, see Fig. 1), nor an evaporation—with original slope $\approx T_1$—from the PLF before full acceleration (in peripheral collisions at Fermi energies the contribution of the Coulomb repulsion to the final PLF velocity is small, while T_2 differs from T_1 by more than a factor of two). Thus one is led to conclude that the particles in the harder component must be attributed to the midvelocity processes. The obtained values of T_2 compare well with those of [22], which however refer to the central part of the midvelocity emissions in a lighter system at higher bombarding energies. Based on Coulomb trajectory calculations, it was shown [3] that in (semi)peripheral collisions particles isotropically emitted on a short time-scale (few tens of fm/c) by a central source (with velocity intermediate between PLF and TLF) are Coulomb-focused in a rather narrow cone, perpendicularly to the PLF-TLF separation axis. In the same paper it was also shown that an appreciable midvelocity contribution in the region schematically indicated in Fig. 1, namely at parallel velocities comparable with that of the PLF, requires that the particles are emitted from an extended source, including a fast contribution of particles emitted nearly at rest in the PLF reference frame, possibly from the PLF surface [3].

What we want to stress here is the remarkable difference between the slopes T_1 and T_2, which is found for all LCPs irrespective of the value (and hence of the selectivity) of the adopted ordering parameter. This fact indicates that the two components always maintain different characteristics. Going toward smaller values of the angle θ in the PLF frame, T_1 does not change, while T_2 shows a weak tendency to decrease, but it remains definitely higher than T_1. At the same time, the percentage of Coulomb-related midvelocity emission

[2]The fit determines B_2 with large uncertainty and there are arguments to expect both a higher (larger Z of the emitter) and a lower (deformed emitter) value than B_1, so we finally use $B_2 = B_1$.

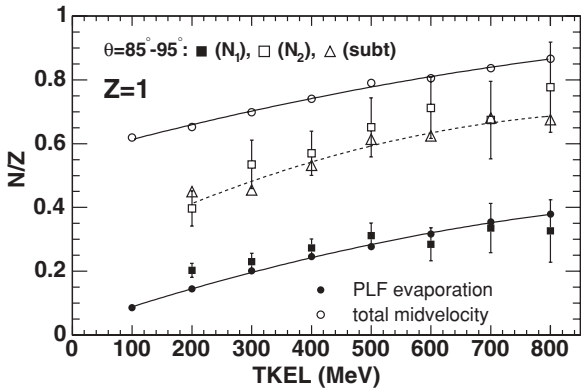

FIG. 4. N/Z ratio for hydrogens as a function of TKEL. Open and full squares refer to the midvelocity and evaporative components, respectively, and are obtained from fits of the kinetic energy spectra at $85^\circ \leqslant \theta \leqslant 95^\circ$ in the PLF frame. Open triangles refer to the midvelocity component in the same angular range and are obtained by subtracting the evaporative component (see text); the dashed line is a quadratic fit to guide the eye. Full and open circles (with full lines) show the results of [5] for evaporation and total midvelocity, respectively.

decreases. Around 90° it amounts to about 25, 50, 60, and 30% of the total emissions of p, d, t, and α, respectively, and it decreases to less than 10% in all cases for $\theta < 40^\circ$.

If the two components observed in the kinetic energy spectra correspond indeed to different production mechanisms, one may expect them to differ also in other properties, like in the average isotopic composition of the emitted particles. For this purpose we have estimated the N/Z ratio of the hydrogen isotopes (for which the detectors have good isotopic resolution) in the angular range $85^\circ \leqslant \theta \leqslant 95^\circ$ in the PLF frame. One can proceed in two different ways. The first one is similar to that adopted in Ref. [5]. One first builds the whole evaporative invariant cross section, $\sigma_{\rm inv}^{\rm evap}(\frac{p_\parallel}{m}, \frac{p_\perp}{m})$, by rotating the part measured in the forward direction so as to fill the whole angular range around the PLF position. Then, one subtracts the so determined $\sigma_{\rm inv}^{\rm evap}$ from the measured total invariant cross section of particles emitted in the forward c.m. hemisphere, $\sigma_{\rm inv}^{\rm tot}$, thus finally obtaining an estimate of the yields of midvelocity emissions of all types. The results are shown by the open triangles in Fig. 4. The second completely different way to proceed is to deduce the average N/Z of the midvelocity emissions directly from the fitted intensity parameter N_2: the results are shown by the open squares in Fig. 4. This second method gives results in agreement with the previous one, although with larger uncertainties. The other fit parameter, N_1, is used for an estimate of the isotopic composition of the evaporative component, shown by the filled squares. Finally, in the same figure, the filled and open circles show the N/Z values obtained in Ref. [5] for the evaporative and total midvelocity emissions, respectively.

The average N/Z for the soft component of the kinetic energy spectra (filled squares) nicely agrees with the value obtained for the evaporation at forward angles (filled circles), thus landing further support to the identification of the soft component (with slope parameter T_1) with an evaporative process. As shown in [5], the experimental values are indeed in close agreement with calculations employing the statistical code GEMINI [23].

For the Coulomb-related part of the midvelocity emissions, the open triangles are in a position intermediate between the open and filled circles at all TKEL. This indicates that this part of the midvelocity emissions, although not as neutron rich as the bulk of the midvelocity emissions from the central "source", nevertheless presents an average isotopic composition definitely higher than that of the usual evaporation (at least for the $Z = 1$ particles). This fact, while confirming a substantial difference between the two mechanisms, may be taken as an indication of a possible enrichment in bound neutrons of "midvelocity" matter [1–3,6,24,25], and/or it might be related to the reduced size of this "source" and hence to its higher energy concentration [4].

In conclusion, we have investigated some aspects of LCPs emitted in peripheral collisions at Fermi energies. We have shown that, still at 90° in the PLF frame, these emissions (with a clear origin from the PLF "source", as manifested by their concentration on the Coulomb ridge [3,5]) consist of two components. The softer component can be identified with the usual evaporation from an equilibrated source, on the basis of both the particle kinetic energies and the N/Z ratio of the hydrogen isotopes. The other component, which displays harder kinetic energy spectra of the particles, shows a more exotic N/Z, with a clear neutron enrichment for bound neutrons with respect to evaporation. These results represent a benchmark against which models describing midvelocity processes should be tested. In any case the presented results are compatible with a picture in which the midvelocity Coulomb-related emission comes from the highly excited contact region between PLF and TLF. After the neck rupture, the PLF may remain partially deformed and locally highly excited; as a consequence, it may tend to evaporate particles and fragments with high kinetic energy and with an isotopic composition resembling that of the neck region, before reaching full equilibration.

[1] J. Łukasik *et al.*, Phys. Rev. C **55**, 1906 (1997).
[2] E. Plagnol *et al.* (INDRA Collaboration), Phys. Rev. C **61**, 014606 (1999).
[3] S. Piantelli *et al.*, Phys. Rev. Lett. **88**, 052701 (2002).
[4] A. Mangiarotti *et al.*, Phys. Rev. Lett. **93**, 232701 (2004).
[5] S. Piantelli *et al.*, Phys. Rev. C **74**, 034609 (2006).
[6] P. M. Milazzo *et al.*, Nucl. Phys. **A703**, 466 (2002).
[7] E. De Filippo *et al.*, Phys. Rev. C **71**, 044602 (2005).
[8] M. Di Toro, A. Olmi, and R. Roy, Eur. Phys. J. A **30**, 65 (2006).
[9] S. Hudan *et al.*, Phys. Rev. C **70**, 031601(R) (2004).
[10] V. Métivier *et al.* (INDRA Collaboration), Nucl. Phys. **A672**, 357 (2000).
[11] J. Łukasik *et al.* (INDRA + ALADIN Collaboration), Phys. Lett. **B566**, 76 (2003).
[12] J. Colin *et al.* (INDRA Collaboration), Phys. Rev. C **67**, 064603 (2003).

[13] A. A. Stefanini *et al*., Z. Phys. A **351**, 167 (1995).
[14] F. Bocage *et al*. (INDRA + NAUTILUS Collaboration), Nucl. Phys. **A676**, 391 (2000).
[15] E. De Filippo *et al*. (REVERSE Collaboration), Phys. Rev. C **71**, 064604 (2005).
[16] M. Jandel *et al*., J. Phys. G **31**, 29 (2005).
[17] M. Bini *et al*., Nucl. Instrum. Methods A **515**, 497 (2003).
[18] G. Casini *et al*., Nucl. Instrum. Methods A **277**, 445 (1989).
[19] Y.-G. Ma *et al*., Phys. Lett. **B390**, 41 (1997).
[20] J. C. Steckmeyer *et al*. (INDRA Collaboration), Nucl. Phys. **A686**, 537 (2001).
[21] E. Vient, Habilit. thesis, University of Caen, France, 2006.
[22] T. Lefort *et al*., Nucl. Phys. **A662**, 397 (2000).
[23] R. J. Charity *et al*., Nucl. Phys. **A483**, 371 (1988).
[24] J. F. Dempsey *et al*., Phys. Rev. C **54**, 1710 (1996).
[25] Y. Larochelle *et al*., Phys. Rev. C **62**, 051602(R) (2000).